

PET imaging of brain with the β -amyloid probe, [^{11}C]6-OH-BTA-1, in a transgenic mouse model of Alzheimer's disease

Hiroshi Toyama^{1, 2}, Daniel Ye³, Masanori Ichise², Jeh-San Liow², Lisheng Cai², David Jacobowitz⁴, John L. Musachio², Jinsoo Hong², Mathew Crescenzo², Dnyanesh Tipre², Jian-Qiang Lu², Sami Zoghbi², Douglass C. Vines², Jurgen Seidel⁵, Kazuhiro Katada¹, Michael V. Green⁵, Victor W. Pike², Robert M. Cohen³, Robert B. Innis²

¹ Department of Radiology, Fujita Health University, 1-98, Dengakugakubo, Kutsukake, Toyoake, 470-1192, Aichi, Japan

² Molecular Imaging Branch, National Institute of Mental Health, National Institutes of Health, Bethesda, Maryland, USA

³ Geriatric Psychiatry Branch, National Institute of Mental Health, National Institutes of Health, Bethesda, Maryland, USA

⁴ Department of Anatomy, Physiology, and Genetics, USUHS, Bethesda, Maryland, USA

⁵ Department of Nuclear Medicine, Warren Grant Magnuson Clinical Center, National Institutes of Health, Bethesda, Maryland, USA

Received: 7 January 2005 / Accepted: 14 February 2005 / Published online: 25 March 2005

© Springer-Verlag 2005

Abstract. *Purpose:* The purpose of this study was to evaluate the capacity of [^{11}C]6-OH-BTA-1 and positron emission tomography (PET) to quantify β -amyloid (A β) plaques in the Tg2576 mouse model of Alzheimer's disease (AD). *Methods:* PET imaging was performed with the NIH ATLAS small animal scanner in six elderly transgenic mice (Tg2576; age 22.0 \pm 1.8 months; 23.6 \pm 2.6 g) overexpressing a mutated form of human β -amyloid precursor protein (APP) known to result in the production of A β plaques, and in six elderly wild-type litter mates (age 21.8 \pm 1.6 months; 29.5 \pm 4.7 g). Dynamic PET scans were performed for 30 min in each mouse under 1% isoflurane inhalation anesthesia after a bolus injection of 13–46 MBq of [^{11}C]6-OH-BTA-1. PET data were reconstructed with 3D OSEM. On the coronal PET image, irregular regions of interest (ROIs) were placed on frontal cortex (FR), parietal cortex (PA), striatum (ST), thalamus (TH), pons (PO), and cerebellum (CE), guided by a mouse stereotaxic atlas. Time–activity curves (TACs) (expressed as percent injected dose per gram normalized to body weight: % ID–kg/g) were obtained for FR, PA, ST, TH, PO, and CE. ROI-to-CE radioactivity ratios were also calculated. Following PET scans, sections of mouse brain prepared from anesthetized and fixative-perfused mice were stained with thioflavin-S.

Results: TACs for [^{11}C]6-OH-BTA-1 in all ROIs peaked early (at 30–55 s), with radioactivity washing out quickly thereafter in both transgenic and wild-type mice. Peak up-

take in all regions was significantly lower in transgenic mice than in wild-type mice. During the later part of the washout phase (12–30 min), the mean FR/CE and PA/CE ratios were higher in transgenic than in wild-type mice (1.06 \pm 0.04 vs 0.98 \pm 0.07, $p=0.04$; 1.06 \pm 0.09 vs 0.93 \pm 0.08 $p=0.02$) while ST/CE, TH/CE, and PO/CE ratios were not. Ex vivo staining revealed widespread A β plaques in cortex, but not in cerebellum of transgenic mice or in any brain regions of wild-type mice.

Conclusion: Marked reductions in brain uptake of this radioligand in transgenic mice may be due to reduced cerebral blood flow relative to that in wild-type mice. Specific [^{11}C]6-OH-BTA-1 binding to A β plaques, if any, is probably very low, as reflected in the small FR/CE and PA/CE ratio differences. FR/CE and PA/CE ratios are considerably higher in AD patients while A β plaque densities in 22-month-old transgenic mice may be expected to show essentially the same density as is observed in the AD brain. This implies that the absence of tracer retention in 22-month-old transgenic mice may be due to the smaller number of A β plaque binding sites and/or to lower affinity of the binding sites for [^{11}C]6-OH-BTA-1 as compared with AD patients. [^{11}C]6-OH-BTA-1 shows excellent brain uptake in mice.

Keywords: Small animal PET – Transgenic mice – [^{11}C]6-OH-BTA-1 – β -Amyloid plaques – Alzheimer's disease

Eur J Nucl Med Mol Imaging (2005) 32:593–600

DOI 10.1007/s00259-005-1780-5

This work was presented at the 51st Annual Meeting of the Society of Nuclear Medicine in Philadelphia, PA, June 19–23, 2004.

Hiroshi Toyama (✉)

Department of Radiology, Fujita Health University, 1-98, Dengakugakubo, Kutsukake, Toyoake, 470-1192, Aichi, Japan
e-mail: htoyama@fujita-hu.ac.jp
Tel.: +81-562-939259, Fax: +81-562-952253

Introduction

Alzheimer's disease (AD) is a neurodegenerative disorder of unknown etiology. The chief features of the disorder are progressive loss of function in multiple cognitive domains,

including memory [1]. Renewed emphasis has been placed on the early diagnosis of AD because commercially available treatments slow the development of impairment but are unable to reverse already present deficits [2]. Minoshima et al. reported that metabolic reductions in the posterior cingulate cortex with topographical analysis of [¹⁸F]2-fluoro-2-deoxy-D-glucose positron emission tomography (FDG-PET) may be a feature of very early AD [3]. Similar findings have been reported for the much more widely available cerebral blood flow single-photon emission computed tomography (SPECT) [4]. However, these findings are not likely to lead to specific diagnostic tests for AD. Currently, a definitive diagnosis of AD can only be established by demonstrating the presence of senile plaques of β -amyloid ($A\beta$) and the neurofibrillary tangles of tau aggregates in the postmortem brain [1]. With respect to the two biological markers, evidence obtained from genetic studies of patients with early-onset familial forms of AD resulting from mutations in the encoding regions of APP and presenilin genes affecting APP processing has focused attention on amyloid plaque formation in Alzheimer pathogenesis [5]. Further, $A\beta$ immunization to reduce $A\beta$ plaques has been proposed as a potentially beneficial treatment for AD [6]. An imaging agent that reflects the amount and distribution of $A\beta$ protein in the brain would be advantageous, particularly because such an agent could be used for specific diagnosis of AD in the presymptomatic stages, when the earliest neuropathologic alterations of AD are present [7]. Recently, PET and SPECT radiotracers with selective affinity for $A\beta$ plaques and with reasonably good image contrast have been developed [8–12]. For example, Klunk et al. have reported a successful PET imaging study in AD patients with [¹¹C]6-OH-BTA-1 (Pittsburgh Compound B or PIB), a tracer that binds to $A\beta$ plaques but not neurofibrillary tangles [13].

Recent advances in PET technology have made it possible to image small animals such as rats and mice [14–17]. PET imaging of mice provides unique opportunities to study the pathophysiology of various disease models, using transgenic manipulation techniques [18]. The major advantage of small animal PET studies over necropsy studies is that the former allow within-subject longitudinal studies [18, 19].

In this study, we evaluated the feasibility of using [¹¹C]6-OH-BTA-1 and a small animal PET scanner for the *in vivo* imaging of $A\beta$ plaques in the Tg2576 mouse model of AD.

Materials and methods

Preparation of [¹¹C]6-OH-BTA-1

[¹¹C]6-OH-BTA-1 was synthesized by a published one-step "loop" method using [¹¹C]methyl triflate [20]. A commercially available loop module (Bioscan, Washington DC), coupled to a GE Petrace MeI Microlab (Milwaukee, WI), was used for the radiolabeling. The radioligand was purified by HPLC on a Phenomenex (Torrance, CA) C18 Prodigy column (10×250 mm, 10 μ m) eluted with acetonitrile/50 mM aqueous triethylammonium phosphate (pH 7.2) (35:65 v/v) at 10 ml/min. [¹¹C]6-OH-BTA-1 (t_R 11 min) was collected, the mobile phase removed by rotary evaporation under reduced pressure and

heat (80°C), and the radiotracer formulated in 2 ml of sterile normal saline containing 5% (v/v) USP grade ethanol. Specific radioactivity (41–118 GBq/ μ mol) at end of synthesis was determined by analytical HPLC (C18 Prodigy, 4.6×250 mm, 10 μ m; 50:50 acetonitrile:50 mM triethylammonium phosphate pH 7.2, 2 ml/min, UV 350 nm, t_R 4.7 min). The radiochemical purity was greater than 95%.

In vitro autoradiographic binding studies using postmortem brains of AD patients and age-matched controls were performed. [¹¹C]6-OH-BTA-1 bound specifically to cortical areas containing $A\beta$ plaques. No specific binding was observed for a control brain specimen.

Animal preparation

All animal procedures were performed in strict accordance with the National Institutes of Health Guide for Care and Use of Laboratory Animals and approved by the National Institute of Mental Health (NIMH) Animal Care and Use Committee.

We evaluated six female transgenic mice (Tg2576; age 22.0±1.8 months; 23.6±2.6 g) overexpressing a mutated form of human β -amyloid precursor protein (APP) known to result in the production of β -amyloid plaques (transgenic mice), and six female wild-type mice from the same litters (age 21.8±1.6 months; 29.5±4.7 g), as confirmed by the polymerase chain reaction method (Table 1).

A 30-G needle (Beckton Dickinson, Franklin Lakes, NJ) attached to a 30-cm polyethylene catheter (dead space ~0.02 ml) was inserted into the tail vein of all mice while awake. The catheters and needles were secured with tissue adhesive (3M Vetbond, St. Paul, MN).

Dynamic PET scans (18 frames; frames 6×20, 5×60, 4×120, 3×300 s) were acquired for 30 min under 1% isoflurane inhalation anesthesia immediately after a bolus injection of 13–46 MBq (Table 1) of [¹¹C]6-OH-BTA-1 (carrier 0.06–0.74 μ g) via the tail vein on the PET scanner bed. We performed dynamic PET scans for 60 min (21 frames; frames 6×20, 5×60, 4×120, 3×300, 3×600 s) for four mice. Body temperature in the anesthetized animals was monitored with a rectal temperature probe and maintained at 36.5–37.5°C with a heating lamp and heating pad.

Small animal PET scanner

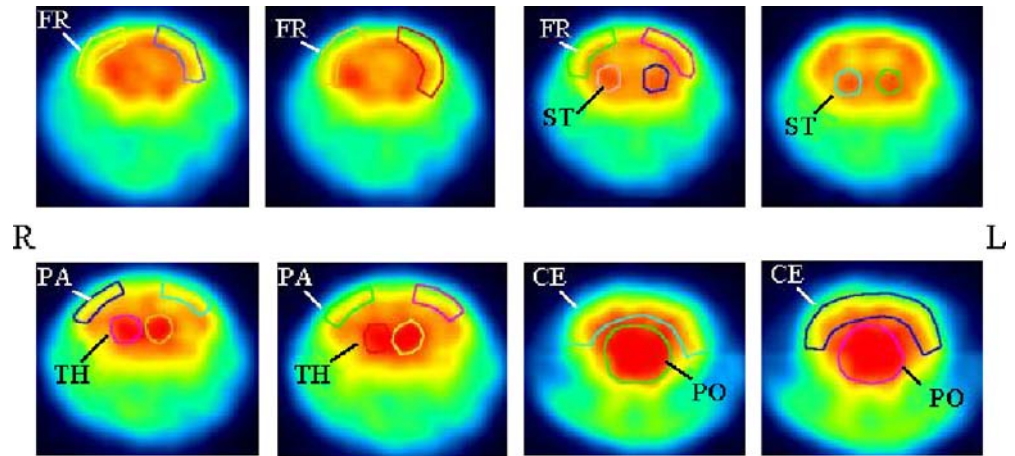
We used the NIH ATLAS (Advanced Technology Laboratory Animal Scanner) PET device with an effective transaxial field of view of 6.0 and a 2-cm axial field of view. The scanner contains 18 dual-layered phoswich detector modules of Ce-doped Lu₁₈Gd_{0.2} (7 mm)/GSO (Ce-doped Gd₂SiO₅) (8 mm) (Hitachi, Japan). This phoswich design allows depth of interaction detection, while preserving a sensitivity of 2.7% (100–650 keV) [21]. PET images were reconstructed with a 3D ordered subset expectation maximization (OSEM) algorithm (ten iterations and 16 subsets), achieving a 1.5-mm full-width at half-maximum resolution at the center [21]. The reconstructed voxel size was 0.56×0.56×1.125 mm. Coronal section images were created for

Table 1. Comparison of transgenic and wild-type mice

	Transgenic mice	Wild-type mice	<i>p</i> value
No.	6	6	
Age (months)	22.0±1.8	21.8±1.6	0.87
Body weight (g)	23.6±2.6	29.5±4.7	0.03*
Injected activity (MBq)	24.4±10.7	21.9±12.6	0.71

**p*<0.05

Fig. 1. ROIs on the summed coronal [^{11}C]6-OH-BTA-1 PET slices in transgenic mouse. R right, L left, FR frontal cortex, ST striatum, PA parietal cortex, TH thalamus, CE cerebellum, PO pons



subsequent data analysis. Image data were not corrected for attenuation or scatter.

PET data analysis

Regions of interest (ROIs) (3–5 mm²) were manually placed over frontal cortex (FR), parietal cortex (PA), striatum (ST), thalamus (TH), pons (PO), and cerebellum (CE) on the summed [^{11}C]6-OH-BTA-1 PET images in mice (Fig. 1). Identification of anatomical structures was guided by the stereotaxic mouse brain atlas (Fig. 1) [22]. These ROIs were copied onto each of the 18 frame images to extract the time-dependent measures. A calibration factor was determined by using a 3-cm diameter cylinder phantom with known activity, enabling ROI counts per pixel to be converted to kilobecquerels per gram tissue, with the assumption that tissue density is 1 g/cm³. These values were divided by the injection dose (kBq) to obtain an image ROI-derived [^{11}C]6-OH-BTA-1 percentage of the injected dose per gram of tissue (% ID/g), and were multiplied by the whole body weight (in kilograms) to determine body weight-normalized radioactivity concentration (% ID-kg/g). The CE was chosen as a reference region because of the absence of thioflavin-S positive A β plaques (see Results). Each ROI to CE ratio was calculated. Differences in % ID-kg/g uptake values in each region at the peak and over the later part of the washout phase (12–30 min) between transgenic and wild-type mice were compared by unpaired *t* tests. Differences in region to CE ratio values over the later part of the washout phase between transgenic and wild-type mice were compared by unpaired *t* tests. The level of statistical significance was designated as $p < 0.05$.

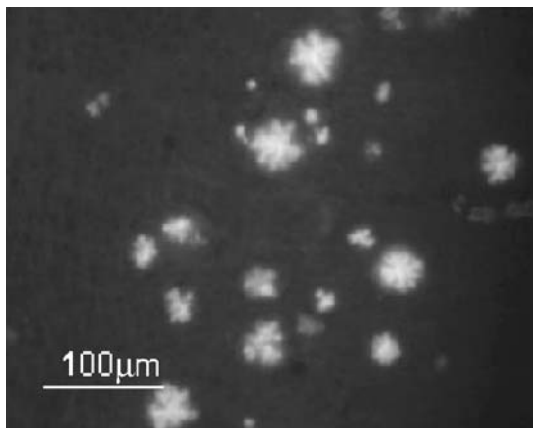


Fig. 2. Fluorescence micrograph of a section of transgenic mouse brain stained with thioflavin-S

Tissue preparation and histochemical staining

On the day following the PET experiment, each animal was anesthetized with pentobarbital (50 mg/kg i.p.) and perfused via the ascending aorta with phosphate buffer solution (PBS), followed by a fixative containing 4% paraformaldehyde in PBS. After perfusion, the brain was quickly removed and immersed in the same fixative for 2 days. The brain was frozen with dry ice and sagittally cut into 15- μm -thick sections with a cryostat. The brain sections were stained with thioflavin-S.

Results

Comparison of transgenic and wild-type mice

There were no significant age differences between transgenic and wild-type mice (Table 1). Body weights of transgenic mice were significantly lower than those of wild-type mice ($p < 0.05$; Table 1).

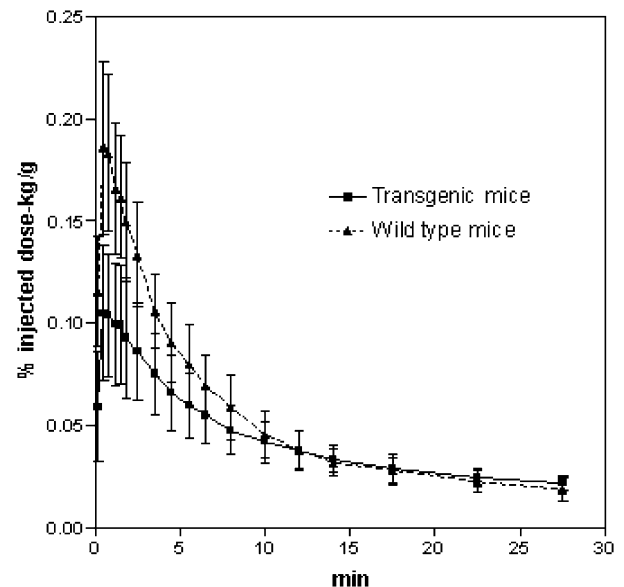


Fig. 3. Representative averaged time-activity curves (\pm SD) of [^{11}C]6-OH-BTA-1 in the frontal cortex

Table 2. [¹¹C]6-OH-BTA-1 peak uptake in each brain region (% ID-kg/g)

	FR	PA	ST	TH	PO	CE
Tg mean (SD)	0.11 (0.03)	0.10 (0.03)	0.13 (0.03)	0.14 (0.04)	0.15 (0.04)	0.11 (0.04)
W mean (SD)	0.19 (0.04)	0.17 (0.03)	0.22 (0.05)	0.23 (0.04)	0.23 (0.04)	0.18 (0.03)
Tg vs W (<i>p</i>)	0.002*	0.002*	0.003*	0.002*	0.01*	0.004*
Tg:W ratio	0.56	0.59	0.58	0.61	0.65	0.58

Tg transgenic mice, W wild-type mice, FR frontal cortex, PA parietal cortex, ST striatum, TH thalamus, PO pons, CE cerebellum
**p*<0.05

Table 3. [¹¹C]6-OH-BTA-1 retention during the later part of the washout phase (12–30 min) in each brain region (% ID-kg/g)

	FR	PA	ST	TH	PO	CE
Tg mean (SD)	0.029 (0.006)	0.029 (0.006)	0.032 (0.006)	0.034 (0.007)	0.036 (0.009)	0.028 (0.006)
W mean (SD)	0.028 (0.007)	0.026 (0.006)	0.035 (0.009)	0.036 (0.009)	0.037 (0.008)	0.028 (0.005)
Tg vs W (<i>p</i>)	0.71	0.46	0.49	0.66	0.48	0.85
Tg:W ratio	1.05	1.10	0.92	0.94	0.91	0.98

Tg transgenic mice, W wild-type mice, FR frontal cortex, PA parietal cortex, ST striatum, TH thalamus, PO pons, CE cerebellum

Histochemical staining of transgenic and wild-type mice

Transgenic mice showed widespread Aβ plaque deposition in cerebral cortex, striatum and thalamus but not in cerebellum (Fig. 2). Wild-type mice showed no Aβ plaque deposition. Figure 2 confirms the presence of Aβ plaques in this animal only; the average plaque density is better understood from published studies showing 42.9 pmol/g tissue at 5 months and 19,937.1 pmol/g tissue at 21 months on average [23].

Comparison of transgenic and wild-type mice PET data

Transgenic and wild-type mice showed rapid entry and clearance of [¹¹C]6-OH-BTA-1 in all regions (Fig. 3). The highest peaks were 0.1±0.02% ID-kg/g (5.0±0.8% ID/g) in transgenic mice and 0.2±0.03% ID-kg/g (7.1±0.9% ID/g) in wild-type mice at between 0.5 and 1.5 min. Peak uptake was significantly lower in all regions in transgenic than in

wild-type mice (Table 2, Fig. 3). There were no significant differences in the averaged % ID-kg/g values over the later part of the washout phase (12–30 min) between transgenic and wild-type mice in each region, including CE (Table 3, Fig. 3). During the later part of the washout phase, the mean FR/CE and PA/CE ratios were higher in transgenic than in wild-type mice (1.06±0.04 vs 0.98±0.07, *p*=0.04; 1.06±0.09 vs 0.93±0.08, *p*=0.02) (Table 4, Figs. 4a and 5). However, the mean ST/CE, TH/CE and PO/CE ratios in the later part of the washout phase were not significantly higher in transgenic than in wild-type mice (Table 4, Figs. 4b and 5).

PET images in transgenic mice

[¹¹C]6-OH-BTA-1 images showed no visually significant difference between uptake in CE and other regions in transgenic and wild-type mice (Fig. 6).

Discussion

In this study, PET imaging in a mouse model of AD with [¹¹C]6-OH-BTA-1 demonstrated excellent brain uptake of radioactivity (peak uptake 0.1–0.2% ID-kg/g) but minimal specific [¹¹C]6-OH-BTA-1 binding to Aβ plaques, as reflected in the small FR/CE and PA/CE ratio differences. To our knowledge, this study is the first to describe results from in vivo Aβ imaging of an AD mouse model using small animal PET. As discussed below, the failure to measure significant in vivo binding to Aβ plaques may be due to the presence of fewer binding sites of Aβ plaques in Tg2576 transgenic mice of this age (as suggested by a literature report [23]), and/or to lower binding affinity of [¹¹C]6-OH-BTA-1 for Aβ plaques in Tg2576 transgenic mice than in AD patients.

Table 4. Region/CE [¹¹C]6-OH-BTA-1 ratios during the later part of the washout phase (12–30 min)

	FR	PA	ST	TH	PO
Tg mean (SD)	1.06 (0.04)	1.06 (0.09)	1.16 (0.10)	1.23 (0.14)	1.28 (0.07)
W mean (SD)	0.98 (0.07)	0.93 (0.08)	1.21 (0.11)	1.24 (0.14)	1.33 (0.07)
Tg vs. W (<i>p</i>)	0.04*	0.02*	0.42	0.78	0.18
Tg:W ratio	1.08	1.14	0.96	0.98	0.94

Tg transgenic mice, W wild-type mice, FR frontal cortex, PA parietal cortex, ST striatum, TH thalamus, PO pons, CE cerebellum
**p*<0.05

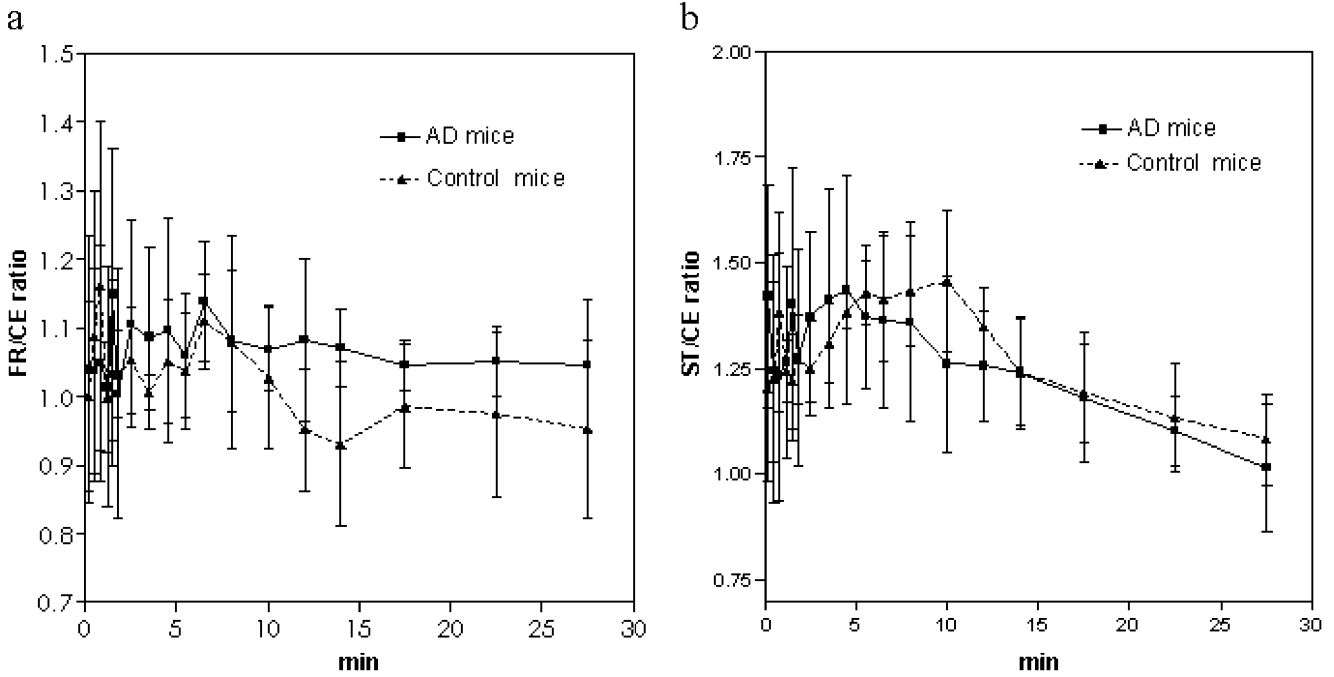


Fig. 4. Averaged time-activity curves (\pm SD) of region/CE $[^{11}\text{C}]6\text{-OH-BTA-1}$ ratios in frontal cortex (a) and striatum (b). *FR* frontal cortex, *ST* striatum, *CE* cerebellum

Mathis et al. reported that in normal mice $[^{11}\text{C}]6\text{-OH-BTA-1}$ entered the brain rapidly (0.21% ID-kg/g at 2 min after intravenous injection) and then cleared rapidly (to 0.018% ID-kg/g at 30 min), these results being based on measurements of dissected brain in a gamma well-counter at each time point. As a measure of radioactivity clearance, the ratio of the 2- to the 30-min % ID-kg/g values was 12:1 [10]. Our averaged peak values (0.21% ID-kg/g) are consistent with their values, which are also very similar to their baboon values (0.27% ID-kg/g) [10]. Average retention values between 12 and 30 min (0.03% ID-kg/g) in the present study are higher than in their study, but our average values between 25 and 30 min (0.019% ID-kg/g, data not

shown) and the ratio of the peak to the 25–30 min % ID-kg/g values (11.1:1) are close to their values [10].

Klunk et al. reported that, compared with healthy control subjects, AD patients showed marked retention of $[^{11}\text{C}]6\text{-OH-BTA-1}$ in areas of the brain known to contain large amounts of amyloid deposits in AD, such as the parietal and frontal cortices [13]. In cortical areas, the mean $[^{11}\text{C}]6\text{-OH-BTA-1}$ standardized uptake value, obtained by normalizing tissue concentration by injected dose and body weight

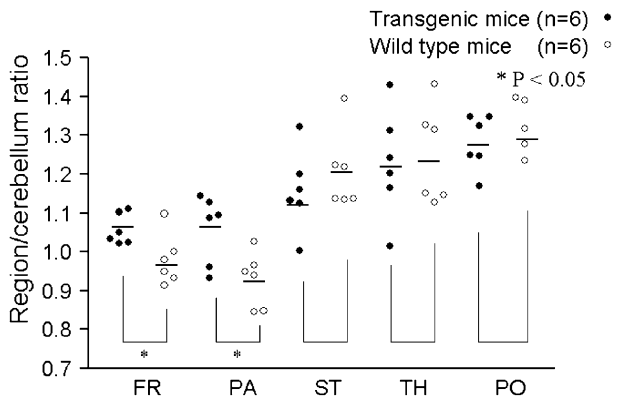


Fig. 5. Comparison of averaged region/CE $[^{11}\text{C}]6\text{-OH-BTA-1}$ ratios during the later part of the washout phase (12–30 min) in transgenic and wild-type mice. *FR* frontal cortex, *PA* parietal cortex, *ST* striatum, *TH* thalamus, *PO* pons

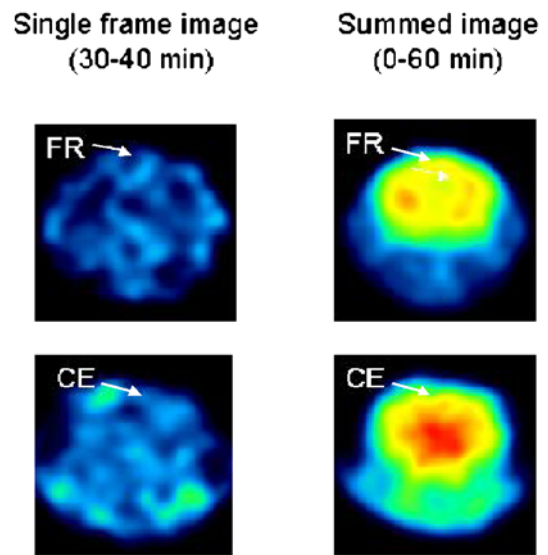


Fig. 6. Representative $[^{11}\text{C}]6\text{-OH-BTA-1}$ coronal PET images of transgenic mouse. *FR* frontal cortex, *CE* cerebellum

during the later part of the washout phase, was significantly higher in AD patients than in control subjects [13]. However, in our study there were no significant differences in the average ID/kg/g values over the later part of the washout phase between transgenic and control mice. Although the mean FR/CE and PA/CE ratios were only slightly higher in transgenic than in wild-type mice in the later part of the washout phase, the effect size was greater than one.

To determine whether the differences between transgenic and wild-type mice in respect of FR/CE and PA/CE ratios are the result of A β plaques in the transgenic mice, studies demonstrating *in vivo* selectivity for these findings would be required. However, it might be reasonable first to attempt to find transgenic mice that show more robust differences from wild-type mice. This might be accomplished either through the use of other AD transgenic models that have a higher A β plaque load or by studying even older Tg2576 animals.

In the interim, it is not unreasonable to speculate that the lower apparent specific [^{11}C]6-OH-BTA-1 binding to A β plaques in elderly transgenic mice as compared with AD patients might be due to either the smaller number or the lower density of A β plaque binding sites in the transgenic mice. Although Terai et al. reported that several characteristics of A β deposits in Tg2576 mouse brains are identical to those in human AD brains, neither significant neuronal loss nor neurofibrillary tangle formation has been reported in this mouse brain [24]. Further, Kalback et al. demonstrated that fundamental structural differences exist between the amyloid characteristic of AD and that deposited in the Tg2576 mice. Thus, differences in disease evolution and biochemistry must be considered when using transgenic animals to evaluate drugs or therapeutic interventions [25].

Kawarabayashi et al. reported that the density of formic acid-extractable A β 42 and A β 40 in Tg2576 mice increases exponentially and substantially from 12 to 23 months, reaching levels similar to those seen in AD brain [23, 26]. A β plaque densities in our 22-month-old mice should be essentially of the same density as is observed in the brains of AD patients. Therefore, it might be more appropriate to emphasize the possibility that absence of tracer retention is caused by the smaller number of binding sites or the lower affinity of the binding sites in Tg2576 mice compared with AD patients, rather than by lower amyloid plaque density. The configuration/folding of A β plaques in Tg2576 mice might be different from the tertiary/quaternary structure of A β plaques in AD brains.

Klunk et al. reported that PS1/APP transgenic mice did not show appreciable retention of [^{11}C]6-OH-BTA-1 in microPET studies. Scatchard analyses suggested that [^{11}C]6-OH-BTA-1 bound to A β with nearly 1:1 molar stoichiometry in AD brain, but binding to synthetic A β showed a much lower stoichiometry of less than 1 mol of [^{11}C]6-OH-BTA-1 bound per 100 mol of A β [27].

Hume and Myers reported that non-tracer kinetics could result if the receptors become saturated with the co-injected stable compound. The degree to which this occurs is dependent on the specific activity of the radiolabelled drug, in

addition to its dissociation constant, and such an event is considered to be especially problematic for neuroreceptor studies using high-affinity, ^{11}C -labelled ligands [28]. The percentage occupancy of A β plaque binding sites by [^{11}C]6-OH-BTA-1 was estimated as follows: Specific activities at the time of injection were 5.3–74.3 GBq/mol. Extrapolating from our PET data, specific binding activities with % ID/g at the later part of washout phase from each injected dose of [^{11}C]6-OH-BTA-1 in transgenic mice were 185–555 kBq/ml in the frontal cortex, which corresponds to 0.35–7.4 pmol/ml of [^{11}C]6-OH-BTA-1 in the frontal cortex. If we presume that the transgenic mice brain A β levels are 20 nmol/g [23, 27], the percentage of occupancy by [^{11}C]6-OH-BTA-1 would be 0.04–0.17%. In this experiment, the tracer dose of [^{11}C]6-OH-BTA-1 (carrier 0.06–0.74 μg) for PET imaging was estimated to result in <0.2% occupancy of A β plaque binding sites. The carrier co-injected in this experiment may not be problematic for tracer kinetics. However, if there are fewer A β plaque binding sites in transgenic mice than in AD brains, percent occupancy of A β plaque binding sites should be increased more.

We have not analysed the possible effects of radiotracer metabolism in mice. Mathis et al. reported that peripheral metabolism of [^{11}C]6-OH-BTA-1 in control mice was rapid, and all of the radiolabeled plasma metabolites of [^{11}C]6-OH-BTA-1 were polar species and were not expected to enter the brain. Radioactivity in the removed brain homogenates indicated very low brain entry of radiolabeled metabolites of [^{11}C]6-OH-BTA-1 and little metabolism of the parent compound in brain parenchyma, consistent with rapid exponential tracer washout from the brain in wild-type mice [10].

It is perhaps somewhat of a surprise that group differences between transgenic and wild-type mice were greater with respect to the initial peak of [^{11}C]6-OH-BTA-1 than with respect to later washout. Decreased peak brain uptake in the transgenic mice, expressed as % ID/kg/g, was partly due to the lower body mass of transgenic compared with wild-type animals. When comparing litter mates of the same species, it is unclear whether there should be correction for body weight. Nevertheless, even when expressed as % ID/g (i.e. without correction for body weight in kg), the average peak uptake in transgenic mice was significantly lower than that in wild-type mice ($5.0 \pm 0.8\%$ ID/g vs $7.1 \pm 0.9\%$ ID/g; $p=0.001$). However, Niwa et al. reported that amyloid precursor protein (APP)–Tg2576 mice aged 2–3 month—an age when no amyloid plaques are present—showed a 25–47% decrease in cerebral blood flow (CBF) measured with the [^{14}C]iodoantipyrine technique and a 18–39% decrease in cerebral glucose utilization measured with the [^{14}C]2-deoxy-D-glucose method as compared with age-matched (APP)–litter mates [29]. If the blood–brain barrier has a high permeability for [^{11}C]6-OH-BTA-1 entry, one would expect the initial brain entry of [^{11}C]6-OH-BTA-1 to be influenced by CBF. The marked reductions in brain uptake of this radioligand in transgenic mice in all regions are consistent with Niwa et al.'s reports. Direct measurements of CBF in the same animals and/or the use of compounds

that will block specific [^{11}C]6-OH-BTA-1 A β plaques should help to clarify this problem and establish appropriate compartmental models for [^{11}C]6-OH-BTA-1 tracer kinetics.

Repeated PET scanning using radiotracers for A β plaque-specific imaging agents in the same transgenic mice might be valuable in evaluating the A β plaque deposition with age. Combined studies with A β plaque-specific imaging agents and a CBF tracer or [^{18}F]FDG to assess cerebral glucose utilization in the same transgenic mice would also be useful.

Since the imaging study in humans with this tracer appeared to be successful [13], our negative results in transgenic mice may not offer insights into the development of imaging agents for human disease. However, our study may contribute to future methodological developments in respect of PET in small animal models.

Conclusion

[^{11}C]6-OH-BTA-1 showed excellent brain uptake in mice. Marked reductions in peak brain uptake of this radiotracer in transgenic mice, compared with wild-type mice, may be due to reduced CBF. Specific [^{11}C]6-OH-BTA-1 binding to A β plaques was probably quite low, if present at all, as reflected in the region/CE ratios. FR/CE and PA/CE ratios are considerably higher in AD patients while A β plaque densities in 22-month-old transgenic mice may be expected to show essentially the same density as is observed in the AD brain. This implies that the absence of tracer retention in 22-month-old transgenic mice may be due to the smaller number of A β plaque binding sites and/or to lower affinity of the binding sites for [^{11}C]6-OH-BTA-1 as compared with AD patients.

Acknowledgements. We thank Dr. Chester A. Mathis, PhD, Department of Radiology, PET Facility, University of Pittsburgh for valuable suggestions.

References

1. Kung HF, Kung MP, Zhuang ZP, Hou C, Lee CW, Plossl K, et al. Iodinated tracer for imaging amyloid plaques in the brain. *Mol Imaging Biol* 2003;5:418–26.
2. Scarpini E, Scheltens P, Feldman H. Treatment of Alzheimer's disease: current status and new perspectives. *Lancet Neurol* 2003; 2:539–47.
3. Minoshima S, Giordani B, Berent S, Frey KA, Foster NL, Kuhl DE. Metabolic reduction in the posterior cingulate cortex in very early Alzheimer's disease. *Ann Neurol* 1997;42:85–94.
4. Kaneko K, Kuwabara Y, Sasaki M, Ogomori K, Ichimiya A, Koga H, et al. Posterior cingulate hypoperfusion in Alzheimer's disease, senile dementia of Alzheimer type, and other dementias evaluated by three-dimensional stereotactic surface projections using Tc-99m HMPAO SPECT. *Clin Nucl Med* 2004;29:362–6.
5. Lee VMY. Taoists and Baptists united—well almost! *Science* 2001;293:1446–7.
6. Schenk D, Barbour R, Dunn W, Gordon G, Grajeda H, Guido T, et al. Immunization with amyloid- β attenuates Alzheimer-disease-like pathology in the PDAPP mouse. *Nature* 1999;400:173–7.
7. Bacskai BJ, Klunk WE, Mathis CA, Hyman BT. Imaging amyloid- β deposits in vivo. *J Cereb Blood Flow Metab* 2002; 22:1035–41.
8. Agdeppa ED, Kepe V, Liu J, Flores-Torres S, Satyamurthy N, Petric A, et al. Binding characteristics of radiofluorinated 6-dialkylamino-2-naphthylethylidene derivatives as positron emission tomography imaging probes for β -amyloid plaques in Alzheimer's disease. *J Neurosci* 2001;21:RC189.
9. Kung M-P, Hou C, Zhuang Z-P, Zhang B, Skovronsky D, Trojanowski JQ, et al. IMPY: an improved thioflavin-T derivative for in vivo labeling of β -amyloid plaques. *Brain Res* 2002;956: 202–10.
10. Mathis CA, Wang Y, Holt DP, Huang G-F, Debnath ML, Klunk WE. Synthesis and evaluation of ^{11}C -labeled 6-substituted 2-arylbenzothiazoles as amyloid imaging agents. *J Med Chem* 2003;46:2740–54.
11. Cai L, Chin FT, Pike VW, Toyama H, Liow JS, Zoghbi SS, et al. Synthesis and evaluation of two ^{18}F -labeled 6-iodo-2-(4 α - $^2-N,N$ -dimethylamino)phenylimidazo[1,2- α]pyridine derivatives as prospective radioligands for β -amyloid in Alzheimer's disease. *J Med Chem* 2004;47:2208–18.
12. Verhoeff NPLG, Wilson AA, Takeshita S, Trop L, Hussey D, Singh K, et al. In-vivo imaging of Alzheimer disease β -amyloid with [^{11}C]SB-13 PET. *Am J Geriatr Psychiatry* 2004;12:584–95.
13. Klunk WE, Engler H, Nordberg A, Wang Y, Blomqvist G, Holt DP, et al. Imaging brain amyloid in Alzheimer's disease with Pittsburgh Compound-B. *Ann Neurol* 2004;55:306–19.
14. Chatzizoiannou AF. Molecular imaging of small animals with dedicated PET tomographs. *Eur J Nucl Med Mol Imaging* 2002; 29 98–114.
15. Green MV, Seidel J, Vaquero JJ, Jagoda E, Lee I, Eckelman WC. High resolution PET, SPECT and projection imaging in small animals. *Comput Med Imaging Graph* 2001;25:79–86.
16. Toyama H, Ichise M, Liow JS, Vines DC, Seneca NM, Modell KJ, et al. Evaluation of anesthesia effects on [^{18}F]FDG uptake in mouse brain and heart using small animal PET. *Nucl Med Biol* 2004;31:251–6.
17. Toyama H, Ichise M, Liow JS, et al. Absolute quantification of regional cerebral glucose utilization in mice by ^{18}F -FDG small animal PET scanning and 2- ^{14}C -DG autoradiography. *J Nucl Med* 2004;45:1398–405.
18. Budinger TF, Benaron DA, Koretsky AP. Imaging transgenic animals. *Annu Rev Biomed Eng* 1999;1:611–48.
19. Cherry SR, Gambhir SS. Use of positron emission tomography in animal research. *I LAR J* 2001;42:219–32.
20. Wilson AA, Garcia A, Chestakova A, Kung H, Houle S. A rapid one-step radiosynthesis of the β -amyloid imaging radiotracer N -methyl- [^{11}C]2-(4'-methylaminophenyl)-6-hydroxybenzothiazole ([^{11}C]6-OH-BTA-1). *J Label Compd Radiopharm* 2004;47: 679–82.
21. Seidel J, Vaquero JJ, Green MV. Resolution uniformity and sensitivity of the NIH ATLAS small animal PET scanner: comparison to simulated LSO scanners without depth-of-interaction capability. *IEEE Trans Nucl Sci* 2003;50:1347–50.
22. Paxinos G, Franklin KBJ. The mouse brain in stereotaxic coordinates. 2nd ed. San Diego: Academic; 2001.
23. Kawarabayashi T, Younkin LH, Saido TC, Shoji M, Ashe KH, Younkin SG. Age-dependent changes in brain, CSF, and plasma amyloid β protein in the Tg2576 transgenic mouse model of Alzheimer's disease. *J Neurosci* 2001;21:372–81.
24. Terai K, Iwai A, Kawabata S, Tasaki Y, Watanabe T, Miyata K, et al. β -amyloid deposits in transgenic mice expressing human β -amyloid precursor protein have the same characteristics as those in Alzheimer's disease. *Neuroscience* 2001;104:299–310.
25. Kalback W, Watson MD, Kokjohn TA, Kuo YM, Weiss N, Luehrs DC, et al. APP transgenic mice Tg2576 accumulate A β peptides that are distinct from the chemically modified and in-

- soluble peptides deposited in Alzheimer's disease senile plaques. *Biochemistry* 2002;41:922–8.
26. Gravina SA, Ho L, Eckman CB, Long KE, Otvos L Jr, Younkin LH, et al. Amyloid β protein ($A\beta$) in Alzheimer's disease brain: biochemical and immunocytochemical analysis with antibodies specific for forms ending at $A\beta$ 40 or $A\beta$ 42(43). *J Biol Chem* 1995;270:7013–6.
27. Klunk WE, Lopresti BJ, Debnath ML, Holt DP, Wang Y, Huang G, et al. Amyloid deposits in transgenic PS1/APP mice do not bind the amyloid PET tracer, PIB in the same manner as human brain amyloid. *Neurobiology of Aging* 2004;25(S2):232.
28. Hume SP, Myers R. Dedicated small animal scanners: a new tool for drug development? *Curr Pharm Des* 2002;8:1497–511.
29. Niwa K, Kazama K, Younkin SG, Carlson GA, Iadecola C. Alterations in cerebral blood flow and glucose utilization in mice overexpressing the amyloid precursor protein. *Neurobiol Dis* 2002;9:61–8.